

Photochemical & Photobiological Sciences

Accepted Manuscript



This is an *Accepted Manuscript*, which has been through the Royal Society of Chemistry peer review process and has been accepted for publication.

Accepted Manuscripts are published online shortly after acceptance, before technical editing, formatting and proof reading. Using this free service, authors can make their results available to the community, in citable form, before we publish the edited article. We will replace this *Accepted Manuscript* with the edited and formatted *Advance Article* as soon as it is available.

You can find more information about *Accepted Manuscripts* in the [Information for Authors](#).

Please note that technical editing may introduce minor changes to the text and/or graphics, which may alter content. The journal's standard [Terms & Conditions](#) and the [Ethical guidelines](#) still apply. In no event shall the Royal Society of Chemistry be held responsible for any errors or omissions in this *Accepted Manuscript* or any consequences arising from the use of any information it contains.

Tyrosine fluorescence probing of the surfactant-induced conformational changes of albumin

Cite this: DOI: 10.1039/x0xx00000x

Nadezda G. Zhdanova^a, Evgeny A. Shirshin^{a,*}, Eugene G. Maksimov^b, Ivan M. Panchishin^a, Alexander M. Saletsky^a and Victor V. Fadeev^a,

Received 00th January 2012,
Accepted 00th January 2012

DOI: 10.1039/x0xx00000x

www.rsc.org/

Tyrosine fluorescence in native proteins is known to be effectively quenched, whereas its emission increases upon proteins' unfolding. This suggests that tyrosine fluorescence could be exploited for probing structural rearrangements of proteins in addition to the extensively used tryptophan emission. We studied the possibility of using tyrosine fluorescence as an indicator of surfactant-induced conformational changes in albumins. It was shown that fluorescence of tyrosine residues, which are uniformly distributed all over the protein molecules, allows detection of subtle structural rearrangements of protein upon surfactant binding, which do not influence on the properties of a single tryptophan residue buried in the inner hydrophobic region of human serum albumin. Tyrosine fluorescence properties, including its fluorescence lifetime, revealed the multistage character of surfactant binding to albumin, consistent with the data provided by other methods. The obtained results demonstrate the possibility of probing conformational changes in proteins using tyrosine photophysical parameters as an indicator.

Introduction

Serum albumins, being the most abundant proteins in blood plasma, are responsible for maintaining osmotic blood pressure¹ and for binding and transport of a wide variety of molecules (drugs, metabolites, fatty acids, *etc.*)¹⁻³. Binding of different ligands by albumin depends not only on the type of ligand but also on the presence of other ligands in solution (competitive binding⁴) as well as on the conformation of the protein molecule⁵.

Albumins have been extensively studied and are now commonly used as model proteins to investigate conformational changes of macromolecules under various external influences (pH, temperature, addition of ligands, *etc.*). Conformational changes of proteins can be monitored using fluorescent probes⁶⁻¹⁰ or intrinsic fluorescence, which is caused by aromatic amino acid residues (tryptophan (Trp), tyrosine (Tyr) and phenylalanine (Phe))¹¹⁻¹⁶.

Among aromatic amino acids, prior attention is paid to Trp because of its high quantum yield in proteins¹⁵ and sensitivity of its fluorescent properties to local environment. For instance,

when a ligand binds to a site on a protein in the vicinity of Trp, a several times decrease of its fluorescence intensity and/or fluorescence lifetime may occur.¹⁵ Moreover, the wavelength of maximum in the fluorescence spectrum of Trp strongly depends on the polarity of its microenvironment.^{17,18} As the result, spectral maximum of Trp fluorescence covers the range from 308 nm (Trp in azurin¹⁹) to 360 nm (Trp in water¹⁵).

Serum albumin is a globular protein, which under physiological conditions adopts a heart-like shape formed by three homologous domains, each of which is further divided in two sub-domains called A and B.¹ In human serum albumin (HSA), the only tryptophan residue (Trp214) is located in the domain II. Two high affinity binding sites (Sudlow I and II) are located near this residue^{20,21}, thus making possible using Trp fluorescence as an indicator of ligand binding to these sites. However, there are other binding sites in HSA (Fig. 1) such as the site for heme in domain I²² and several fatty acids binding sites that are located far from Trp 214^{23,24}. As the result, conformational changes of HSA caused by binding of these ligands may have no significant influence on Trp microenvironment and, consequently, its fluorescence signal

may remain unchanged. In this case, specific fluorescent labels which are sensitive to the conformational changes in the vicinity of ligand binding sites are used.²⁵ Another approach is the use of homologous proteins, *e.g.* bovine serum albumin (BSA), which has an additional tryptophan residue (Trp134) located in the domain I.^{1,15,26}

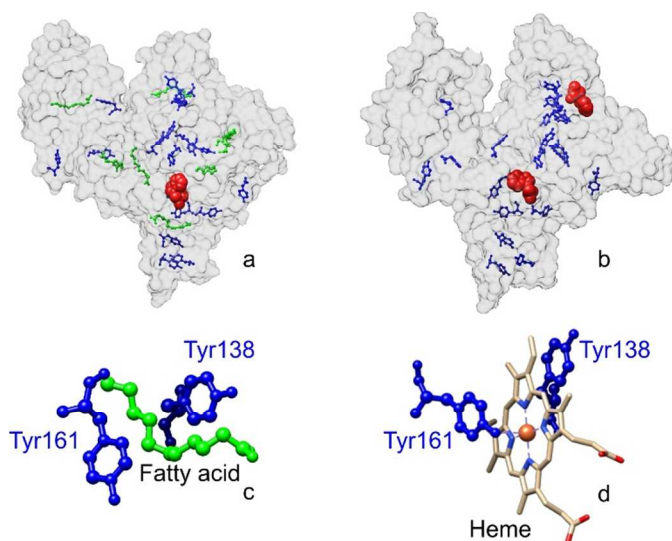


Figure 1. a) Structure of the complex HSA-fatty acid (pdb ID: 1ef7²³, Tyr – blue, Trp – red, fatty – green). b) Structure of BSA (pdb ID: 3v03²⁶, Tyr – blue, Trp – red). The binding site in the domain I of HSA formed by pi-stacked Tyr138 and Tyr161²⁷ c) in complex HSA – fatty acid (pdb ID: 1ef7²³) and d) in complex HSA-heme (pdb ID: 1n5u²²). The pictures were prepared using the USCF Chimera package²⁸.

Proteins conformational changes can be studied using different denaturing agents, among which surfactants are probably the most extensively used. At low concentrations of surfactant in solution it acts as a ligand and its binding is determined by the presence of several specific sites in protein macromolecule, while at high concentrations surfactant appears to be a denaturing agent.²⁹ The complex non-monotonous dependence of binding affinity on the concentration of surfactant makes it a convenient model for the investigation of a wide range of conformational changes in proteins including subtle changes due to binding to the high affinity sites at ligand low concentrations and dramatic alterations of protein's structure at high concentrations.¹⁰

Comparison of binding of surfactant to BSA and HSA based on Trp fluorescence demonstrates a significant difference between these homologous albumins at its low concentrations (1 - 10 surfactant molecules per protein molecule).^{13,14,30} This fact was interpreted by the difference in mutual location of tryptophan residues (Trp214 in HSA and Trp134 and Trp213 in BSA) and the high affinity binding sites in HSA and BSA.

Here, we made use of tyrosine residues (Tyr) fluorescence in albumin to obtain additional information about conformational changes of albumin caused by its interaction with ionic surfactant (sodium dodecyl sulfate, SDS). Tyr fluorescence in proteins is usually quenched due to (i) ionization of the residue by neighbor amino or carboxyl groups^{1,15,31} or (ii) excitation

energy transfer to tryptophan^{6,31-36}. At the same time, several works³¹⁻³⁹ demonstrate that protein denaturation may lead to Tyr fluorescence enhancement due to structural rearrangements leading to the elimination of quenching mechanisms mentioned above. This suggests that ligand binding to protein, if leading to conformational changes, may result in the reduction of Tyr fluorescence quenching efficiency, *e.g.* by increasing the distance between certain tyrosine and tryptophan residues. We also note that Tyr is distributed in serum albumins more uniformly than Trp (Fig. 1) because of its higher content (18 vs 1 for HSA and 20 vs 2 for BSA), hence, Tyr could possibly be a sensitive probe of conformational changes of protein's segments located far from Trp.

In this work, we studied the behaviour of intrinsic fluorescence of BSA and HSA, caused by both Tyr and Trp, upon surfactant binding. We showed that the dependence of Tyr fluorescence on surfactant concentration was similar for the investigated proteins (BSA and HSA), while Trp fluorescence exhibited significant differences. We also investigated the Tyr microenvironment by means of 4th derivative absorption spectroscopy⁴⁰⁻⁴⁴ and picosecond time-resolved fluorescence spectroscopy¹⁵. The obtained results revealed the surfactant concentration range corresponding to the changes in intramolecular energy transfer efficiency from Tyr to Trp residues and showed that optical parameters of Tyr may provide new information about conformational changes in protein upon both ligand binding and denaturation.

Results and discussion

1. Fluorescence of tryptophan (Trp) and tyrosine (Tyr) residues. Comparison between BSA and HSA

The dependence of Trp fluorescence intensity on SDS concentration obtained upon 295 nm excitation for HSA and BSA is presented in Fig. 2. For both proteins, four stages were observed in fluorescence quenching, that is a well-known fact in fluorescence spectroscopy of albumin-surfactant systems^{29,45-47}. Essentially, this multistage character of protein-surfactant interaction is manifested in other physical parameters of this system, such as surface tension⁴⁸⁻⁵², calorimetric titration data²⁹, conductometric titration data⁴⁷, *etc.* Different stages of interaction exhibit a rich variation of cooperativity, binding energy (and, consequently, interaction mechanism and type of binding sites) and influences on protein's secondary and tertiary structure.²⁹ We will use the upper scheme, presented in Fig. 2, which illustrates our current understanding of the albumin-SDS interaction based on the literature data^{7,8,10,11,12,14,29}, to interpret the changes of fluorescence upon titration. In Fig. 2, SDS molecules are marked with green circles, SDS binding sites on albumin in yellow circles, and tryptophan residues with red circles.

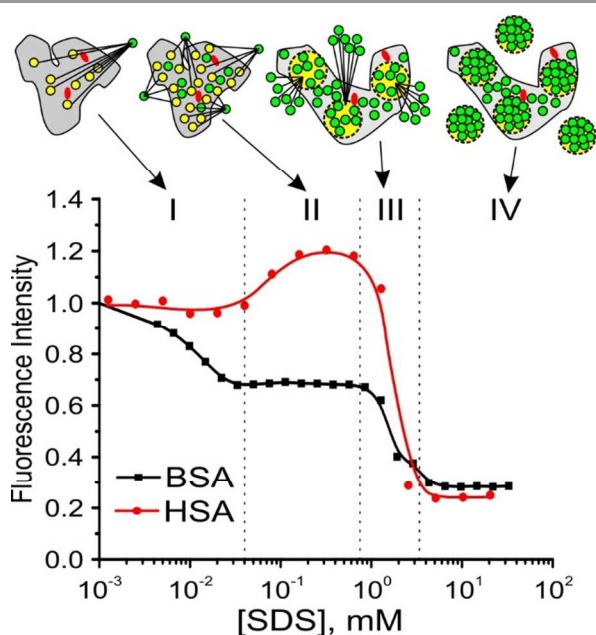


Figure 2. Maximum fluorescence intensity of BSA (black squares) and HSA (red circles) as a function of SDS concentration, $\lambda_{\text{exc}} = 295$ nm. BSA and HSA concentrations were $4.7 \mu\text{M}$ and $4.1 \mu\text{M}$, respectively. Maximum fluorescence intensity was normalized to the value obtained at $[\text{SDS}] = 0$. The description of the binding stages corresponding to different SDS concentration regions is given in the text.

At low SDS concentrations (region I) the fluorescence of HSA was almost constant, while that of BSA decreased to *ca* 70% of the initial value. Gelamo and co-workers^{13,14} explained this difference by the presence of primary quencher binding sites in the vicinity of the Trp134 located in the domain I in BSA, while such sites are absent in the neighbourhood of the internal tryptophan residue in albumin (Trp214 in HSA and Trp213 in BSA, located in the domain II). This interpretation used the analogy between the binding of myristic acid and surfactant to albumin. It is considered that no changes in secondary structure of albumin occur during this binding stage^{11,52,53}, while subtle rearrangements in tertiary structure are revealed in Trp fluorescence^{11,12,14}.

Further, an increase in intensity for Trp in HSA was observed, while fluorescence of BSA was constant (region II). This fact was explained by Gelamo and Tabak¹⁴ as the consequence of the reduction of Trp214 static fluorescence quenching in HSA by neighbouring groups, which is present in the native structure. The same situation should hold for Trp213 in BSA, and the lack of fluorescence enhancement in this case could be the consequence of the compensation between Trp134 fluorescence quenching and Trp213 fluorescence enhancement. During the next stage, formation of micelle-like aggregates on proteins' backbone leads to a sharp decrease in the fluorescence intensity of both HSA and BSA (region III, see the scheme in Fig. 2). This stage is connected with global rearrangements of albumin's structure as indicated by circular dichroism, SAXS and EPR data.^{29,47,52,53} After that, the saturation of proteins structure with surfactant molecules occurred and no changes of

fluorescence signal were observed for both HSA and BSA (region IV, see the scheme in Fig. 2).

Hereby, comparison between the binding of surfactant molecules to BSA and HSA based only on Trp fluorescence showed significant difference at low SDS concentrations (*ca* 1 - 10 molecules of SDS per a protein molecule): fluorescence intensity of HSA did not change while in the case of BSA it decreased gradually. HSA and BSA contain one and two Trp residues, respectively. At the same time, the number of tyrosine residues is 18 for HSA and 20 for BSA, hence, the distribution of Tyr in proteins structure is more uniform compared to Trp (see Fig. 1a,b). This fact suggests that Tyr fluorescence, if detectable, can provide additional information about ligand binding to sites located far from tryptophan residues.

The spectral contribution of Tyr can be obtained from protein spectra excited at 280 nm (when both Tyr and Trp are excited) and at 295 nm (where Tyr absorption is negligible and only Trp is excited). Assuming the fluorescence band shape of Trp to be independent on the excitation wavelength, it is possible to obtain Tyr parameters from spectra.³⁷ The fluorescence spectra of BSA ($\lambda_{\text{exc}}=280$ nm) obtained in absence of SDS and at maximum SDS concentration (32.8 mM), as well as their deconvolution into the individual spectra of Tyr and Trp, are presented in Fig. 3.

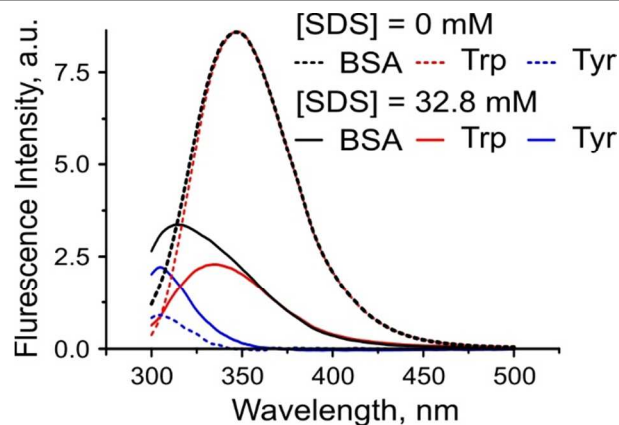


Figure 3. Fluorescence spectra of BSA (black lines) and contributions of Tyr (blue lines) and Trp (red lines) with (solid lines) and without SDS (dashed lines); $\lambda_{\text{exc}}=280$ nm, BSA concentration was $4.8 \mu\text{M}$.

Fluorescence spectra of albumin obtained at high SDS concentrations at $\lambda_{\text{exc}} = 280$ nm exhibited the spectral maximum close to that of free Tyr (308 nm, see Fig. 3). This effect is often observed for denatured proteins and is interpreted as the consequence of Tyr-Trp energy transfer reduction³¹⁻³⁹. Hence, considering the stepwise unfolding of albumin upon SDS binding and the shift of fluorescence maximum at $\lambda_{\text{exc}} = 280$ nm to the spectral maximum of free tyrosine in aqueous solution, one could expect the gradual increase in Tyr fluorescence.

The normalized fluorescence intensity of Tyr ($\lambda_{\text{exc}} = 280$ nm) as a function of surfactant concentration for BSA and HSA is presented in Fig. 4. The dependence of Tyr fluorescence on SDS concentration is similar for both proteins, suggesting that

surfactant binding in these homologous proteins is similar. The dependence in Fig. 4 also exhibits four characteristic stages similar to that observed for the Trp fluorescence (Fig. 2), but in case of Tyr emission enhancement is observed upon SDS binding.

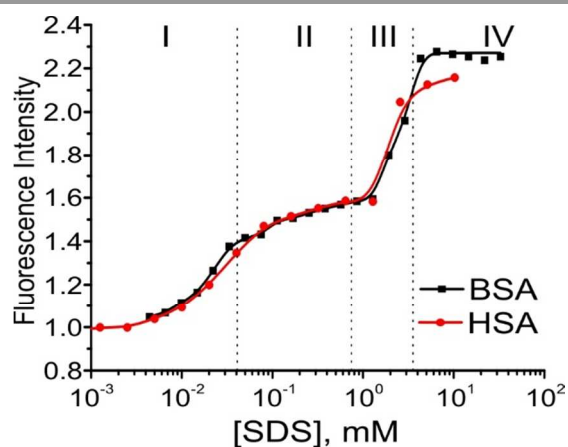


Figure 4. Maximum fluorescence intensity of Tyr for BSA (black squares) and HSA (red circles) as a function of SDS concentration, $\lambda_{\text{exc}} = 280$ nm. Concentrations of BSA and HSA were $4.7 \mu\text{M}$ and $4.1 \mu\text{M}$, respectively. Maximum fluorescence intensity was normalized to the value obtained at $[\text{SDS}] = 0$.

Figure 5 shows the variation of Trp and Tyr fluorescence characteristics for BSA upon SDS binding. As mentioned above, in the region I ($[\text{SDS}] = 9 \cdot 10^{-3} - 4 \cdot 10^{-2}$ mM) no global alterations of protein's structure occur, hence, the polarity of Trp microenvironment remained constant and no shift in the position of fluorescence maximum was observed (Fig. 5a). At the same time, simultaneous quenching of Trp fluorescence and enhancement of Tyr emission were detected (Fig. 5). In this region, corresponding to 1-10 SDS molecules per protein, binding to the specific (high affinity) sites occurs which is mainly due to electrostatic interactions.^{13,29,52} We consider that in this region of SDS concentrations the reduction of Tyr fluorescence quenching is likely to be caused by the decrease in the efficiency of energy transfer to Trp, since the subtle alterations of protein structure during this binding stage are not expected to be enough to remove the quenching by amino groups located in the vicinity of Tyr residues.

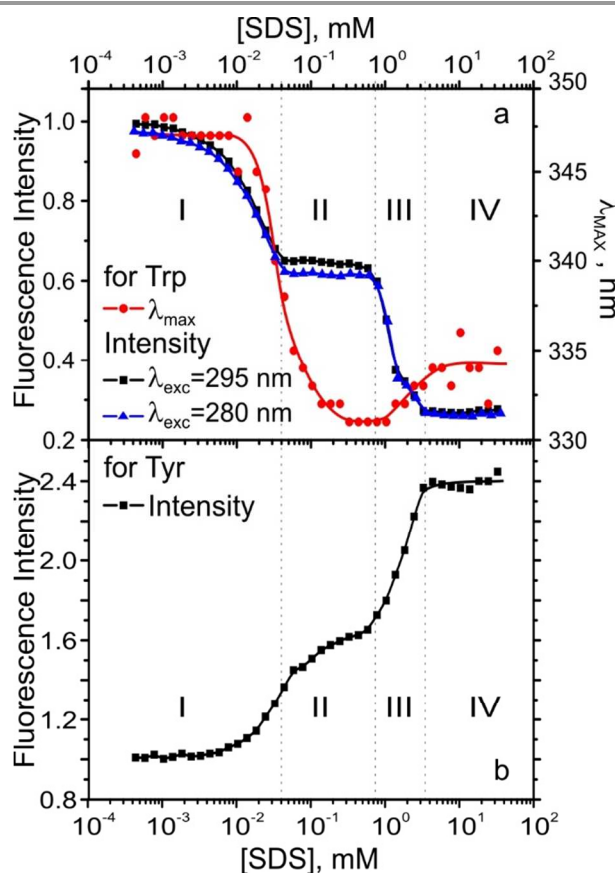


Figure 5. a) Maximum fluorescence intensity of Trp in BSA ($\lambda_{\text{exc}} = 295$ nm – black squares, $\lambda_{\text{exc}} = 280$ nm – blue triangles) and position of its spectral maxima λ_{max} (red circles) as a function of SDS concentration ($\lambda_{\text{exc}} = 295$ nm). b) Maximum fluorescence intensity of Tyr in BSA as a function of SDS concentration, $\lambda_{\text{exc}} = 280$ nm. BSA concentration was $4.8 \mu\text{M}$. Maximum fluorescence intensity was normalized to the value obtained at $[\text{SDS}] = 0$.

The region I is followed by the region II ($[\text{SDS}] = 4 \cdot 10^{-2} - 0.7$ mM, 10-150 SDS/BSA), which is characterized by the plateau in Trp fluorescence as a function of SDS concentration accompanied by the blue shift of its maximum, indicating the decrease of the polarity of Trp microenvironment and by the slight increase of Tyr fluorescence (Fig. 5). In the region II SDS molecules bind to the low affinity sites which became available due to conformational changes in proteins structure on the stage I, and binding of SDS molecules to BSA is driven mainly by hydrophobic interactions.^{11,29,52}

A strong quenching of Trp fluorescence accompanied by a slight red shift of its maximum and a sharp increase of Tyr fluorescence intensity take place in the region III ($[\text{SDS}] = 0.7 - 3$ mM, SDS/BSA = 150 - 625) which corresponds to the formation of micelles in the buffer solution used in the experiment (see Fig. 5 and the scheme in Fig. 2). The binding stage in the surfactant concentration region, corresponding to critical micelle concentration, is characterized by a high level of cooperativity.²⁹ For instance, a high level of binding cooperativity in the region III for the albumin-SDS system was demonstrated by Anand *et al.*¹¹ using the modified Stern-Volmer plot, which provided the slope of the fluorescence quenching curve on the double logarithmic scale $n = 3.13$.

Though this parameter is usually interpreted in literature as the number of binding sites, it was shown⁵⁴⁻⁵⁶ that this interpretation is erroneous and the value n is only capable of indicating the degree of binding cooperativity. The albumin-SDS system perfectly illustrates this suggestion – independent assessment of bound SDS molecules n_{SDS} in the region III of concentration provided n_{SDS} close to 100^{14,29} that greatly exceeds the value obtained from the modified Stern-Volmer plots ($n = 3.13$ obtained by Anand *et al.*¹¹). Interestingly, the value $n = 3.13$ is the highest one obtained from the modified Stern-Volmer plots we found in literature⁵⁵.

As the result of SDS binding during the reported stage, micelle-like aggregates of surfactant molecules are formed on proteins backbone (see the scheme in Fig. 2, region III). The presence of these aggregates led to the increase of Trp microenvironment polarity that was manifested in a *ca* 3 nm red shift of fluorescence maximum and to the removal of quenching of Tyr fluorescence (Fig. 5). The latter could be the consequence of global rearrangements of proteins structure, which could lead both to the reduction of Tyr-Trp energy transfer³¹⁻³⁹ and the removal of Tyr quenching by neighboring amino groups.

In the last region IV ($[\text{SDS}] > 3$ mM) protein backbone is saturated with micelle-like aggregates and new SDS molecules form free micelles in solution, consequently, binding of new SDS molecules to BSA did not occur and no changes in fluorescence properties of both Tyr and Trp fluorescence were observed.

2. Fourth derivative absorption spectroscopy

To obtain information about changes in the vicinity of amino acids from absorption spectrum of a protein, the derivative absorption spectroscopy was proposed by Fell⁴¹. The 4th derivative of absorption spectrum of a protein is a good compromise between the improvement of the resolution of peaks and the decrease of signal/noise ratio.^{40,43,57,58} To investigate Tyr environment, the following characteristics of the 4th derivative of absorption spectra of a protein are usually used^{43,44,59}:

(i) the position of the peak λ_2 , which corresponds to the 0-0 transition of the phenol ring of Tyr (Fig. 6),

(ii) the ratio R , which is determined as:

$$R = \frac{I(\lambda_2) - I(\lambda_4)}{I(\lambda_1) - I(\lambda_3)} = \frac{p_1}{p_2}, \quad (1)$$

where

$$I(\lambda_i) = \frac{\delta^4 A}{\delta \lambda^4}(\lambda_i)$$

are the values of calculated 4th derivative of absorption spectra at λ_i ; $\lambda_{1,2}$ and $\lambda_{3,4}$ are wavelength of its local maxima and local minima, shown in Fig. 6.

The ratio R strongly depends on the heterogeneity of Tyr residue's environment – the higher is R , the more uniform is the environment of Tyr residues – and exhibits only a weak dependence on the presence of the hydrogen bond formed by OH-group of Tyr residue.^{43,59} On the contrary, the parameter λ_2 characterizes the mentioned hydrogen bond and is weakly influenced by the heterogeneity of the environment of Tyr residues.

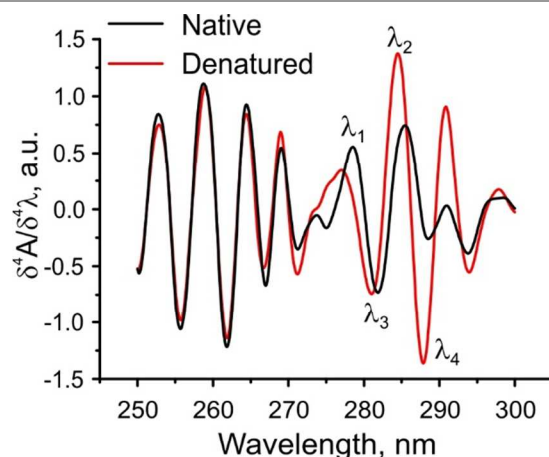


Figure 6. The 4th derivative of absorption spectra of BSA (4.8 μM) in its native ($[\text{SDS}] = 0$) and denatured ($[\text{SDS}] = 32.86$ mM) forms. The description of the parameters λ_1 , λ_2 , λ_3 , λ_4 shown in the figure, is provided in the text.

As it can be seen in Fig. 7, at the first two stages of BSA-SDS interaction (region I and II, $[\text{SDS}] = 9 \cdot 10^{-3} - 0.7$ mM) polarity of Tyr residue is almost constant upon SDS binding. This fact suggests that there are no binding sites for SDS near Tyr residues for this range of ligand concentrations. Within region III both R and λ_2 dramatically change, indicating perturbation in the vicinity of Tyr residues due to SDS binding. The same fact was observed by Ning *et al.*⁴², and it was concluded that the polarity of Tyr microenvironment increases and hydrogen bond by OH-group of Tyr forms upon SDS binding within region III due to formation of micelle-like aggregates on the protein backbone. This observation is in agreement with global structural rearrangements of albumins structure in the region III of SDS concentrations mentioned above.

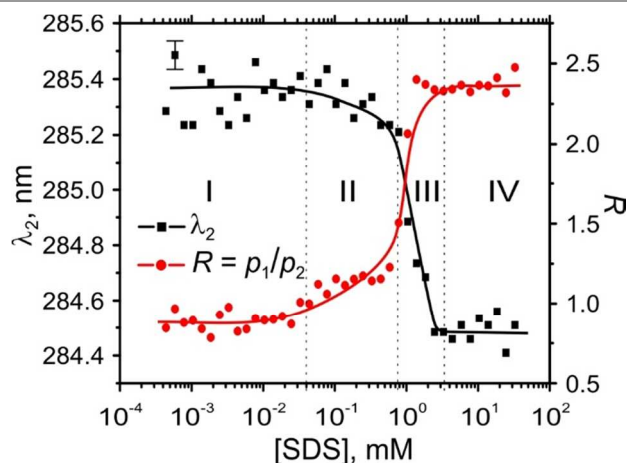


Figure 7. Parameters λ_2 (black squares) and R (red circles) of the 4th derivative absorption spectra of BSA as a function of SDS concentration. BSA concentration was 4.8 μM .

3. Time-resolved fluorescence measurements and the determination of fluorescence lifetimes for Trp and Tyr

Fluorescence decay of Tyr and Trp fluorescence was measured using a custom-built spectrofluorimeter. Trp fluorescence decay at the wavelength λ_{Trp} (ca 355 nm) corresponding to the fluorescence maximum of the native protein was fitted by a sum of two exponential decay functions. Biexponential nature of Trp fluorescence decay in BSA is usually explained by the presence of two tryptophan residues in different environments.^{13,14,60,61} At the same time, fluorescence decay of free tryptophan in aqueous solution is also biexponential due to the presence of rotamers.^{11,62-66}

Fluorescence decay obtained at λ_{Trp} was characterized by the mean lifetime (Fig. 8, black squares) which exhibited the dependence on SDS concentration similar to that for Trp intensity (Fig. 5a, black squares). This fact suggested that the quenching of Trp fluorescence was caused by additional non-radiative relaxation pathways induced by SDS binding to protein molecules and is in agreement with literature¹¹.

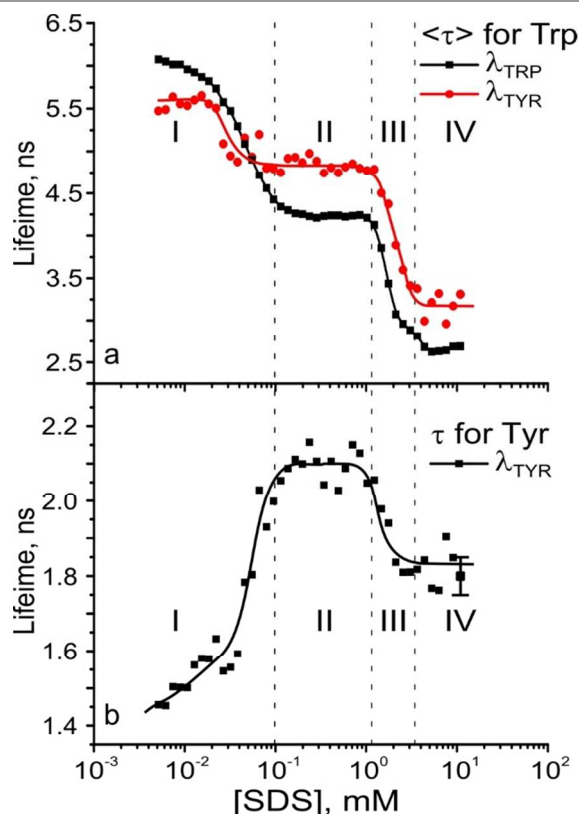


Figure 8. a) Mean fluorescence lifetime for Trp obtained at registration wavelength λ_{Trp} (ca 355 nm) (black squares) and λ_{Tyr} (ca 318 nm) (red circles) as a function of SDS concentration, $\lambda_{\text{exc}} = 280$ nm. b) Fluorescence lifetime for Tyr obtained at the registration wavelength λ_{Tyr} (ca 318 nm) as a function of SDS concentration, $\lambda_{\text{exc}} = 280$ nm. The concentration of BSA was 3.5 μM .

BSA fluorescence decay at λ_{Tyr} (spectral maxima of Tyr fluorescence for steady-state experiments, ca 310 nm) was

fitted by a sum of three exponential decays. Two longer lifetimes depended on SDS concentration similar to that for Trp fluorescence lifetime obtained at λ_{Trp} , thus we attributed these two values to Trp fluorescence. Fig. 8a demonstrates the comparison between the mean fluorescence lifetimes of Trp obtained from decay curves at different registration wavelengths (λ_{Tyr} and λ_{Trp}) as a function of SDS concentration. A slight overestimation of the mean fluorescence lifetime for shorter registration wavelength was probably caused by the presence of long decay component due to smaller signal/noise ratio (*i.e.*, lower sensitivity of the detector and lower signal from Trp at λ_{Tyr}).

The shortest lifetime component obtained at λ_{Tyr} as a function of SDS concentration was very different from the others, corresponding to Trp (Fig. 8b). Based on this difference between the fluorescence lifetimes obtained at λ_{Tyr} , we concluded that the shortest lifetime corresponded to Tyr fluorescence decay. This allowed separate detection of the lifetime components of fluorescence decay of BSA for Trp and Tyr despite their spectral overlap. Abou-Zied and Al-Shihi⁶ studied HSA unfolding in the presence of guanidine hydrochloride (GdnHCl), and showed the appearance of Tyr peak at 280 nm excitation upon protein's denaturation. This fact was interpreted as the consequence of the reduction Tyr-263 to Tyr-214 energy transfer efficiency caused by HSA unfolding. However, Abou-Zied and Al-Shihi⁶ indicated that the separate determination of Tyr and Trp fluorescence lifetimes is very difficult due to their proximity and dynamic processes occurring during the excited state lifetime. In our experiments, the behavior of fluorescence decay at two wavelengths, one of which corresponds to the maximum of Trp emission in the native protein (355 nm) and the other close to tyrosine emission maximum in BSA (318 nm) was investigated. No increase in fluorescence lifetimes was observed at the registration wavelengths where Tyr emission was negligible and the emission was solely due to Trp residues ($\lambda > 300$ nm). This fact led us to the conclusion that the shortest fluorescence decay component at λ_{Tyr} , which exhibited an increase upon SDS addition consistent with the increase in Tyr fluorescence obtained from the steady-state experiments, belonged to Tyr.

In the region I of SDS concentrations the polarity of Tyr microenvironment was constant, while the increase of fluorescent intensity and lifetime was similar as a function of SDS concentration. Moreover, literature data^{11,52,53} suggest that no changes in secondary structure of albumin occur during this binding stage, and fluorescence variations are caused by subtle alterations of tertiary structure. These alterations led to the enhancement of Tyr fluorescence intensity (Fig. 5) and lifetime (Fig. 8b) and did not influence the polarity of Tyr (Fig. 7).

4. The mechanisms of Tyr fluorescence enhancement upon the unfolding of BSA

Tyrosine fluorescence in proteins is a common topic in proteins spectroscopy. It was shown⁶⁷ that in tryptophan-containing protein Tyr fluorescence is not observed, that led to the

suggestion about the effective Tyr-Trp energy transfer. The Foerster radius for the Tyr-Trp pair is ~ 10 - 18 Å, that is comparable to typical distances between these residues in proteins.⁶⁸ At the same time, fluorescence quantum yield of Tyr in proteins containing no tryptophan residues is also very low compared to aqueous solution, suggesting that Tyr fluorescence is quenched by the neighbouring amino acids, *e.g.*, by nearby charged amino or carboxylate groups^{67,68}.

Tyr fluorescence usually increases upon protein denaturation and transition to random coil, and the changes in its fluorescence were suggested^{39,67,69} to be due to alterations in proteins tertiary structure. A number of works deal with the Tyr-Trp energy transfer^{32,35,37,38,39,67-70}, for instance, the method for the estimation of the efficiency of excitation energy transfer (EET) from Tyr to Trp based on the comparison of quantum yield at 280 and 295 nm excitation, was proposed³⁵. Interestingly, contradictory results were obtained for the Tyr-Trp energy transfer efficiency in different works for some proteins as described by Vekshin *et al.*⁷² These facts suggests that the role of Tyr-Trp energy transfer in quenching of tyrosine fluorescence in proteins might be overestimated.

Our results clearly show the increase of Tyr fluorescence upon SDS binding and protein unfolding (including the stage where the secondary structure is supposed to be unaltered, corresponding to the region I of SDS concentrations). This is in agreement with the general concept presented in literature⁶⁸, which suggests the increase of Tyr fluorescence in proteins occurs upon its unfolding. It was also shown (Fig. 5a-b) that the changes in Tyr fluorescence in albumin exhibits the multistaged character, typical for the surfactant-protein interaction. Figure 5a demonstrates that the decrease in Trp fluorescence upon SDS binding by BSA is similar at 280 and 295 nm excitation. In case of strong Tyr-Trp EET this would not be the case – Trp fluorescence at 280 nm excitation would exhibit a more rapid decrease due to the reduction of an additional EET-related excitation efficiency. The absence of such differences suggests that Tyr-Trp EET is not the dominating process in Tyr fluorescence quenching in albumin.

The results of time-resolved measurements indicated the increase of Tyr lifetime on the first binding stage (Fig. 8b), that is consistent with the reduction of some quenching pathways efficiency. However, on the stage III, corresponding to the micelles formation SDS concentration region (see the scheme in Fig. 2), the decrease of Tyr lifetime was observed, while the steady-state intensity showed an increase (Fig. 5b). We also note that dramatic changes in Tyr microenvironment were observed on this stage as revealed by the 4th derivative absorption spectroscopy (Fig. 6). Hence, the inconsistency between the opposite trends in Tyr fluorescence intensity and fluorescence lifetime changes on the third binding stage could possibly be explained by the changes in Tyr absorption spectrum. The 4th derivative of absorption spectra showed a blue shift in the area, corresponding to Tyr absorption, on the third stage of SDS binding (Fig. 6), suggesting the increase of Tyr /absorption cross-section at 280 nm. Interactions between amino acid residues in protein may result in the hypochromic

effect (the reduction of absorption coefficient) and spectral shift.^{70,71} The degree of these interactions, and, consequently, the changes in absorption spectrum, could be expected to vary depending on the protein structural rearrangement, that are mostly pronounced on the third binding stage.

5. Application of Tyr fluorescence to albumin-ligand complex and related conformational changes

We demonstrated that the binding of SDS to BSA and HSA results in similar changes Tyr fluorescence, suggesting that surfactant binding is identical for the investigated proteins. It was also confirmed that Trp fluorescence of the investigated proteins changes in different manner upon SDS binding. The difference in steady-state fluorescence of Trp in BSA and HSA as a function of SDS concentration seems to be caused by changes in the vicinity of the additional Trp in BSA (Trp134), *i.e.* high affinity SDS binding sites exist in the domain I of BSA. Hence, the comparative study of ligand binding to BSA and HSA using fluorescence of both Tyr and Trp could possibly allow one to obtain information about ligand binding to the domain I of HSA without external labels.

The proposed method of using Tyr fluorescence as the indicator of ligand binding to the domain I can be applied for (i) divalent metal ions⁷²⁻⁷⁷, which are considered to bind to the domain I, (ii) porphyrin-related molecules (PPIX, heme, phtalocyanines *etc.*)^{22,78,79}. In the latter case, the intrinsic fluorescence of the protein (Tyr and Trp contributions) can be considered as a complementary source of information about ligand binding to optical characteristics of ligands themselves (structured absorption and fluorescence spectra). The X-ray data (pdb ID: 1n5u²²) indicated that the heme binding site consists of two stacked Tyr residues (Tyr138 and Tyr161, see Fig. 1d). Recent QM/MM modelling of the absorption spectrum of HSA²⁷ demonstrated the essential role of electronic coupling in two pairs of stacked Tyr residues, one of which coincides with the Tyr138-Tyr161 couple. This suggests that the binding of a ligand into this site could interfere the interaction between the stacked tyrosine residues, resulting in the changes of both absorption and fluorescence spectra of albumin.

Based on these examples, we propose that a variety of intermolecular interactions, including small ligands binding, could influence photophysical processes involving tyrosine residues in albumin, resulting in changes of Tyr fluorescence. From this perspective, the approach applied in this work seems to be a promising tool for conformational changes probing.

Experimental

1. Materials

Bovine serum albumin (BSA, fatty acid free, Sigma-Aldrich, USA), human serum albumin (HSA, fatty acid free, Sigma-Aldrich, USA), sodium dodecyl sulfate (SDS, Sigma-Aldrich, USA), Tris-(hydroxymethyl)-aminomethane (Tris, Dia-M, Russia) were used as obtained without further purification. All

solutions were prepared using bidistilled water. Tris-HCl buffer (0.1 M) was used to maintain pH at 7.40 ± 0.05 . All measurements were performed at room temperature (25 ± 1 °C) without temperature stabilization.

Protein concentrations were determined spectrophotometrically using known extinction coefficients at 280 nm ($4.4 \cdot 10^4$ M⁻¹ cm⁻¹ and $3.5 \cdot 10^4$ M⁻¹ cm⁻¹ for BSA and HSA, respectively)¹. Sequential dilution of the protein-surfactant solution with the solution of protein of the same concentration was used to obtain the dependence of fluorescence parameters on SDS concentration. The concentrations of protein for each experiment are presented in the text.

2. Determination of critical micelle formation concentration (CMC) for Tris-buffer

Pyrene fluorescence (the ratio of the intensities of the first peak (373 nm) in fluorescence spectrum to the third one (384 nm)) was used to determine the critical micelle concentration (CMC) of SDS in Tris-HCl buffer (0.7 mM, see ESI).⁸⁰

3. UV absorption

Absorption spectra were measured using Lambda 25 spectrophotometer (Perkin-Elmer) in the 250 - 500 nm wavelength region. The bandwidth of both slits was set to 1 nm, the increment was 1 nm, the scanning rate was 960 nm/min.

4. Steady-state fluorescence

Fluorescence spectra were measured with Fluoromax-4 (Horiba Jobin Yvon). Two excitation wavelengths λ_{exc} were used to excite proteins intrinsic fluorescence: 280 nm (both Tyr and Trp were excited) and 295 nm (only Trp was excited). Fluorescence emission was measured in the 300 - 500 nm wavelength region, the bandwidths of both slits were set to 2 nm.

The position of the spectral maximum for Trp fluorescence ($\lambda_{exc} = 295$ nm) λ_{max} was determined after the spectra smoothing procedure based on Savitzky-Golay algorithm⁵⁸ using a filter window of 21 points and the polynomial degree of four. The smoothing procedure increased the accuracy of determination of λ_{max} .

Each fluorescence spectrum was the average of three measurements.

5. Tyrosine (Tyr) fluorescence

Deconvolution of the spectra obtained at $\lambda_{exc} = 280$ nm was performed to obtain Tyr emission spectra. For this purpose, normalized Trp fluorescence spectra obtained at $\lambda_{exc} = 295$ nm were subtracted from the fluorescence spectra obtained $\lambda_{exc} = 280$ nm which represented the sum of Tyr and Trp emission. It was assumed that the band shape of Trp fluorescence did not depend on the excitation wavelength³⁷. The detailed procedure of Tyr fluorescence evaluation can be found elsewhere^{31,37,38}. The Raman emission of water was negligible compared to both Trp and Tyr fluorescence (ESI, Fig. S1), hence, it was not taken

into account when performing the deconvolution procedure. We note that the error of the deconvolution procedure didn't exceed 1.1% of maximum of Tyr emission.

6. Fourth derivative UV-absorption spectra

Fourth-derivative absorption spectra were calculated using the Savitzky-Golay algorithm^{40,58,59,81} with the filter window as small as possible (9 points). The calculated 4th derivative spectra were interpolated using cubic spline to improve the resolution of peaks to 0.05.⁴²

7. Time-resolved fluorescence

Fluorescence lifetime measurements were performed using the custom-built fluorimeter. The setup consisted of a photomultiplier system with a Hamamatsu R5900 16-channel multi-anode photomultiplier (PML-16, Becker&Hickl, Berlin, Germany). The polychromator was equipped with 600 grooves/mm grating resulting in a spectral bandwidth of the PML-16 of 200 nm (resolution of 12.5 nm/channel). Excitation was performed with a pulsed 280 nm light-emitting diode (Edinburgh Instruments, UK) delivering 700 ps FWHM, average power 0.8 μ W pulses at a repetition rate of 10 MHz. Data acquisition for all time-resolved measurements of protein solutions was performed during 30 s to obtain the optimum signal for the deconvolution procedure.

Fluorescence decay curves for Trp fluorescence were obtained using the channel corresponding to the wavelength λ_{Trp} (*ca* 355 nm) which is the closest to the fluorescence emission maximum of the native protein. It was assumed that the possible contribution of the Tyr fluorescence at this wavelength was negligible. The minimum value of residual for the fluorescence decay of Trp was achieved by approximation using a sum of two exponential decay functions. Fluorescence decay at the channel corresponding to the wavelength λ_{Tyr} (*ca* 318 nm) was analyzed as well, since this wavelength was close to the maximum of fluorescence of Tyr (*ca* 308 nm) and had an appropriate value of the signal/noise ratio (the sensitivity of the detector at lower wavelengths was insufficient). The minimum value of residual at this channel was achieved by using a sum of three exponentials.

The average fluorescence lifetime for Trp residues at each wavelength was calculated according to the expression:

$$\langle \tau \rangle = \frac{\sum_i \tau_i a_i}{\sum_i a_i}, \quad (2)$$

where τ_i and a_i are the lifetime and the amplitude (normalized to unity) of the *i*th fluorescence decay component attributed to Trp, respectively.

Representative fluorescence decay curves for BSA and its approximation; statistical data (χ^2), fluorescence lifetimes and its relative amplitudes for fitting of decays are presented in the ESI.

Conclusions

Here, sequential changes in Tyr photophysical properties of albumins upon surfactant binding were investigated using the 4th derivative absorption spectroscopy, steady-state and time-resolved fluorescence spectroscopy. In the latter case, an approach allowing separate detection of Tyr and Trp fluorescence lifetimes in albumin was suggested. The changes in optical properties of Tyr revealed the four stage character of SDS binding by albumin, which is consistent with the data obtained from tryptophan fluorescence and literature data, obtained by other physical methods. On the first binding stage (1-10 SDS molecules per protein), when binding to the high-affinity sites occurs and only subtle structural rearrangements of albumin take place, a similar increase in steady-state intensity and fluorescence lifetime of Tyr was obtained for both BSA and HSA. Interestingly, on this binding stage no changes in fluorescence of a single tryptophan residue buried in the inner hydrophobic region of HSA were observed, suggesting that fluorescence of tyrosine residues, which are uniformly distributed all over the protein molecules, is a more sensitive indicator of conformational changes in this case. Next, on the third binding stage, corresponding to the SDS concentration range where micelles formation takes place, simultaneous increase in Tyr fluorescence intensity and decrease of its fluorescence lifetimes were observed. This fact was interpreted as the consequence of the changes in Tyr absorption caused by hypochromic effects (*i.e.*, blue shift of absorption band to the changes in protein's conformation), that is in agreement with an abrupt change of Tyr microenvironment on this binding stage as revealed by the 4th derivative absorption spectroscopy. Finally, the similar change of tryptophan fluorescence intensity upon SDS binding at 280 and 295 nm excitation suggested that excitation energy transfer from tyrosine to tryptophan residues is not the predominant mechanism of Tyr fluorescence quenching in albumin. We consider that the obtained results demonstrate the possibility of probing conformational changes in proteins using tyrosine photophysical parameters as an indicator, and the suggested approach can be successfully applied to other protein-ligand systems, thus providing a spectroscopic tool in addition to classical tryptophan fluorescence.

Acknowledgements

The reported study was supported by Russian Scientific Foundation (grant 14-15-00602).

Molecular graphics and analyses were performed with the UCSF Chimera package²⁸. Chimera is developed by the Resource for Biocomputing, Visualization, and Informatics at the University of California, San Francisco (supported by NIGMS P41-GM103311).

Notes and references

^a Department of Physics, M.V. Lomonosov Moscow State University, Moscow 119991, Russia.

^b Department of Biology, M.V. Lomonosov Moscow State University, Moscow 119991, Russia.

* Corresponding author: shirshin@lid.phys.msu.ru.

Electronic Supplementary Information (ESI) available: comparison of Raman emission from water and fluorescence of BSA; representative fluorescence decay curves for BSA and its approximation; statistical data

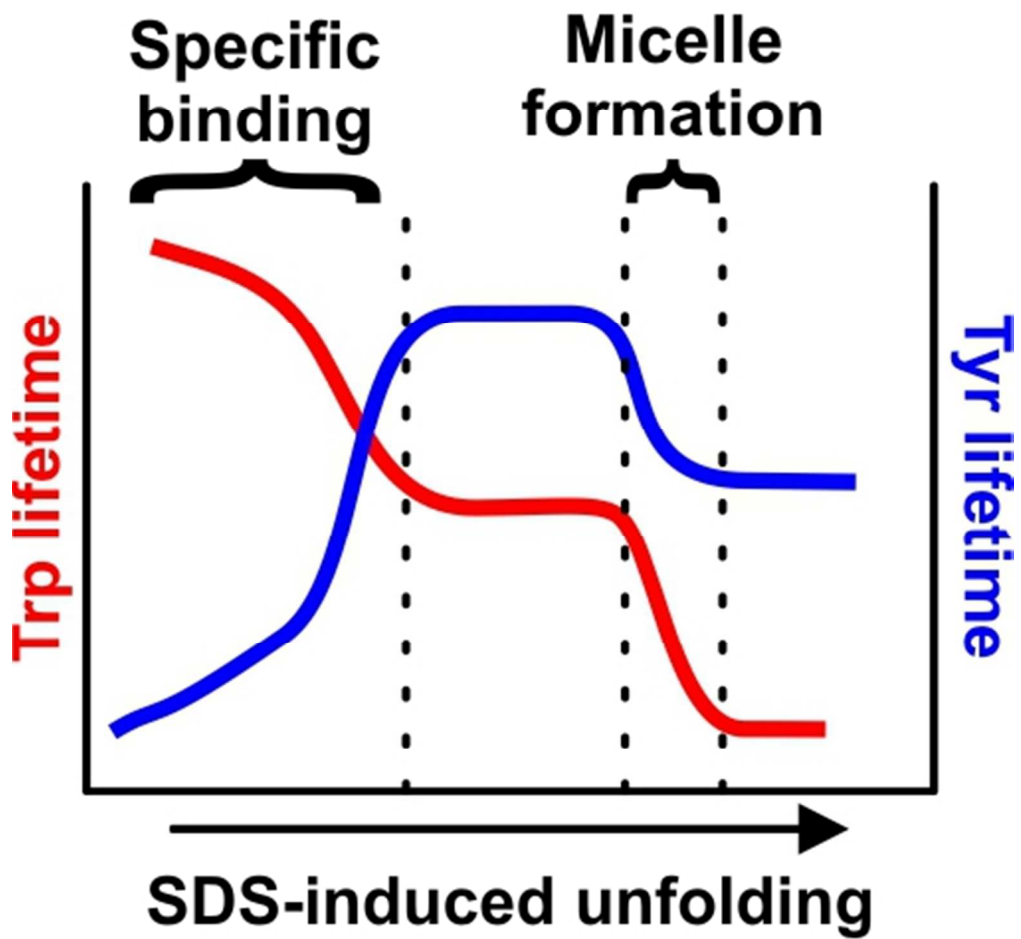
(χ^2), lifetimes and its relative amplitudes for fitting of decays; determination of critical micelle concentration for SDS in Tris-buffer by means of pyrene (Py) fluorescence. See DOI: 10.1039/b000000x/

1. T. J. Peters, Serum Albumin, *Adv. Protein Chem.*, 1985, **37**, 161-245. DOI: 10.1016/S0065-3233(08)60065-0.
2. S. Curry, Lessons from the Crystallographic Analysis of Small Molecule Binding to Human Serum Albumin, *Drug Metab. Pharmacokin.*, 2009, **24** (4), 342-357. DOI: 10.2133/dmpk.24.342.
3. A. Varshney, P. Sen, E. Ahmad, M. Rehan, N. Subbarao and R.H. Khan, Ligand Binding Strategies of Human Serum Albumin: How Can the Cargo Be Utilized?, *Chirality*, 2010, **22** (1), 77-87. DOI: 10.1002/chir.20709.
4. A. Sułkowska, M. Maciążek-Jurczyk, B. Bojko, J. Równicka, I. Zubik-Skupień, E. Temba, D. Pentak and W.W. Sułkowski, Competitive Binding of Phenylbutazone and Colchicine to Serum Albumin in Multidrug Therapy: a Spectroscopic Study, *J. Mol. Struct.*, 2008, **881** (1-3), 97-106. DOI: 10.1016/j.molstruc.2007.09.001.
5. I. Petitpas, A.A. Bhattacharya, S. Twine, M. East and S. Curry, Crystal Structure Analysis of Warfarin Binding to Human Serum Albumin. Anatomy of Drug Site I, *J. Biol. Chem.*, 2001, **276**, 22804-22809. DOI: 10.1074/jbc.M100575200.
6. O. K. Abou-Zied and O. I. K. Al-Shihi, Characterization of Subdomain IIA Binding Site of Human Serum Albumin in its Native, Unfolded, and Refolded States Using Small Molecular Probes, *J. Am. Chem. Soc.*, 2008, **130** (32), 10793-10801. DOI: 10.1021/ja8031289.
7. P. Hazra, D. Chakrabarty, A. Chakraborty and N. Sarkar, Probing Protein-Surfactant Interaction by Steady State and Time-Resolved Fluorescence Spectroscopy, *Biochem. Biophys. Res. Commun.*, 2004, **314** (2), 543-549. DOI: 10.1016/j.bbrc.2003.12.118.
8. A. Samanta, B. K. Paul and N. Guchhait, Spectroscopic Probe Analysis for Exploring Probe-Protein Interaction: a Mapping of Native, Unfolding and Refolding of Protein Bovine Serum Albumin by Extrinsic Fluorescence Probe, *Biophys. Chem.*, 2011, **156** (2-3), 128-139. DOI: 10.1016/j.bpc.2011.03.008.
9. A. Sharma, P. K. Agarwal and S. Deep, Characterization of Different Conformations of Bovine Serum Albumin and Their Propensity to Aggregate in the Presence of N-cetyl-N,N,N-trimethyl Ammonium Bromide, *J. Colloid Interface Sci.*, 2010, **343** (2), 454-462. DOI: 10.1016/j.jcis.2009.12.012.
10. N. Turro, X. Lei, K. P. Ananthapadmanabhan and M. Aronson, Spectroscopic Probe Analysis of Protein-Surfactant Interactions: the BSA/SDS System, Spectroscopic Probing of the Microenvironment in a Protein-Surfactant Assembly, *Langmuir*, 1995, **11** (7), 2525-2533. DOI: 10.1021/la00007a035.
11. U. Anand, C. Jash and S. Mukherjee, Spectroscopic Probing of the Microenvironment in a Protein-Surfactant Assembly, *J. Phys. Chem. B*, 2010, **114** (48), 15839-15845. DOI: 10.1021/jp106703h.
12. U. Anand and S. Mukherjee, Binding, Unfolding and Refolding Dynamics of Serum Albumins, *Biochim. Biophys. Acta, Gen. Subj.*, 2013, **1830** (12), 5394-5404. DOI: 10.1016/j.bbagen.2013.05.017.
13. E. L. Gelamo, C. H. T. P. Silva, H. Imasato and M. Tabak, Interaction of Bovine (BSA) and Human (HSA) Serum Albumins with Ionic Surfactants: Spectroscopy and Modelling, *Biochim. Biophys. Acta, Protein Struct. Mol. Enzymol.*, 2002, **1594** (1), 84-99. DOI: 10.1016/S0167-4838(01)00287-4.

14. E. L. Gelamo and M. Tabak, Spectroscopic Studies on the Interaction of Bovine (BSA) and Human (HSA) Serum Albumins with Ionic Surfactants, *Spectrochim. Acta, Part A*, 2000, **56** (11), 2255-2271. DOI: 10.1016/S1386-1425(00)00313-9.
15. J. Lakowicz, *Principles of Fluorescence Spectroscopy*, Springer, New York, 3rd edn., 2007.
16. E. Lissi, E. Abuin, M. E. Lanio and C. Alvarez, New and Simple Procedure for the Evaluation of the Association of Surfactants to Proteins, *J. Biochem. Biophys. Methods*, 2002, **50** (2-3), 261-268. DOI: 10.1016/S0165-022X(01)00237-8.
17. P. R. Callis, Molecular Orbital Theory of the 1L_b and 1L_a States of Indole *J. Chem. Phys.*, 1991, **95** (6), No. 4230. DOI: 10.1063/1.460778.
18. J. T. Vivian and P. R. Callis, Mechanisms of Tryptophan Fluorescence Shifts in Proteins, *Biophys. J.*, 2001, **80** (5), 2093-2109. DOI: 10.1016/S0006-3495(01)76183-8.
19. E. A. Burstein, N. S. Vedenkina and M. N. Ivkova, Fluorescence and the Location of Tryptophan Residues in Protein Molecules, *Photochem. Photobiol.*, 1973, **18** (4), 263-279. DOI: 10.1111/j.1751-1097.1973.tb06422.x.
20. D. J. Birkett, S. P. Myers and G. Sudlow, Effects of Fatty Acids on Two Specific Drug Binding Sites on Human Serum Albumin, *Mol. Pharmacol.*, 1977, **13** (6), 987-992.
21. G. Sudlow, D. J. Birkett and D. N. Wade, Further Characterization of Specific Drug Binding Sites on Human Serum Albumin, *Mol. Pharmacol.*, 1976, **12** (6), 1052-1061.
22. M. Wardell, Z. Wang, J. X. Ho, J. Robert, F. Ruker, J. Ruble and D. C. Carter, The Atomic Structure of Human Methemalbumin at 1.9 Å, *Biochem. Biophys. Res. Commun.*, 2002, **291** (4), 813-819. DOI: 10.1006/bbrc.2002.6540.
23. A. A. Bhattacharya, T. Grune and S. Curry, Crystallographic Analysis Reveals Common Modes of Binding of Medium and Long-Chain Fatty Acids to Human Serum Albumin, *J. Mol. Biol.*, 2000, **303** (5), 721-732. DOI: 10.1006/jmbi.2000.4158.
24. S. Curry, H. Mandelkow, P. Brick and N. Franks, Crystal Structure of Human Serum Albumin Complexed with Fatty Acid Reveals an Asymmetric Distribution of Binding Sites, *Nat. Struct. Biol.*, 1998, **5**, 827-835. DOI: 10.1038/1869.
25. B. Ahmad, M. Z. Ahmed, S. K. Haq and R. H. Khan, Guanidine Hydrochloride Denaturation of Human Serum Albumin Originates by Local Unfolding of Some Stable Loops in Domain III, *Biochim. Biophys. Acta, Proteins Proteomics*, 2005, **1750** (1), 93-102. DOI: 10.1016/j.bbapap.2005.04.001.
26. K. A. Majorek, P. J. Porebski, A. Dayal, M. D. Zimmerman, K. Jablonska, A. J. Stewart, M. Chruszcz and W. Minor, Structural and Immunologic Characterization of Bovine, Horse, and Rabbit Serum Albumins, *Mol. Immunol.*, 2012, **52** (3-4), 174-182. DOI: 10.1016/j.molimm.2012.05.011.
27. T. Etienne, X. Assfeld and A. Monari, QM/MM Calculation of Absorption Spectra of Complex Systems: The Case of Human Serum Albumin, *Comput. Theor. Chem.*, 2014, **1040-1041**, 360-366. DOI: 10.1016/j.comptc.2014.01.009.
28. E. F. Pettersen, T. D. Goddard, C. C. Huang, G. S. Couch, D. M. Greenblatt, E. C. Meng and T. E. Ferrin, UCSF Chimera—a Visualization System for Exploratory Research and Analysis, *J. Comput. Chem.*, 2004, **25** (13), 1605-1612.
29. D. Otzen, Protein-Surfactant Interactions: A Tale of Many States, *Biochim. Biophys. Acta, Proteins Proteomics*, 2011, **1814** (5), 562-591. DOI: 10.1016/j.bbapap.2011.03.003.
30. Y. Moriyama, D. Ohta, K. Hachiya, Y. Mitsui and K. Takeda, Fluorescence Behavior of Tryptophan Residues of Bovine and Human Serum Albumins in Ionic Surfactant Solutions: a Comparative Study of the Two and One Tryptophan(s) of Bovine and Human Albumins, *J. Protein Chem.*, 1996, **15** (3), 265-272. DOI: 10.1007/BF01887115.
31. R. B. Weinberg, Exposure and Electronic Interaction of Tyrosine and Tryptophan Residues in Human Apolipoprotein A-IV, *Biochemistry*, 1988, **27** (5), 1515-1521. DOI: 10.1021/bi00405a018.
32. R. F. Borkman and S. R. Phillips, Tyrosine-to-Tryptophan Energy Transfer and the Structure of Calt Gamma-II Crystallin, *Exp. Eye Res.*, 1985, **40** (6), 819-826. DOI: 10.1016/0014-4835(85)90127-7.
33. S. Gorinstein, I. Goshev, S. Moncheva, M. Zemser, M. Weisz, A. Caspi, I. Libman, H. T. Lerner, S. Trakhtenberg and O. Martin-Belloso, Intrinsic Tryptophan Fluorescence of Human Serum Proteins and Related Conformational Changes, *J. Prot. Chemistry*, 2000, **19** (8), 637-642. DOI: 10.1023/A:1007192017291.
34. D. Li, D. Hong, H. Guo, J. Chen and B. Ji, Probing the Influences of Urea on the Interaction of Sinomenine With Human Serum Albumin by Steady-State Fluorescence, *J. Photochem. Photobiol. B*, 2012, **117**, 126-131. DOI: 10.1016/j.jphotobiol.2012.09.007.
35. Y. Saito, H. Tachibana, H. Hayashi and A. Wada, Excitation-Energy Transfer Between Tyrosine and Tryptophan in Proteins Evaluated By the Simultaneous Measurement of Fluorescence and Absorbance, *Photochem. Photobiol.*, 1981, **33** (3), 289-295. DOI: 10.1111/j.1751-1097.1981.tb05420.x.
36. J. Steinhardt, J. Krijn and J. G. Leidy, Differences Between Bovine and Human Serum Albumins: Binding Isotherms, Optical Rotatory Dispersion, Viscosity, Hydrogen Ion Titration, and Fluorescence Effects, *Biochemistry*, 1971, **10** (22), 4005-4015. DOI: 10.1021/bi00798a001.
37. M. Eisenhawer, S. Cattarinussi, A. Kuhn and H. Vogel, Fluorescence Resonance Energy Transfer Shows a Close Helix-Helix Distance in the Transmembrane M13 Procoat Protein, *Biochemistry*, 2001, **40** (41), 12321-12328. DOI: 10.1021/bi0107694.
38. Eisinger, J. Feuer, B. and A. A. Lamola, Intramolecular Singlet Excitation Transfer. Applications to Polypeptides, *Biochemistry*, 1969, **8** (10), 3908-3915. DOI: 10.1021/bi00838a005.
39. M. J. Kronman and L. G. Holmes, The Fluorescence of Native, Denatured and Reduced-Denatured Proteins, *Photochem. Photobiol.*, 1971, **14** (2), 113-134. DOI: 10.1111/j.1751-1097.1971.tb06157.x.
40. M. R. Bray, A. D. Carriere, and A. J. Clarke, Quantification of Tryptophan and Tyrosine Residues in Proteins by Fourth-Derivative Spectroscopy, *Anal. Biochem.*, 1994, **221** (2), 278-284. DOI: 10.1006/abio.1994.1412.
41. A. F. Fell, The Analysis of Aromatic Amino Acids by Second and Fourth Derivative UV-Spectroscopy, *J. Pharm. Pharmacol.*, 1979, **31** (S1), No. 23P. DOI: 10.1111/j.2042-7158.1979.tb11571.x.
42. A.-M. Ning, L. Meng, Z.-L. Zhao, X.-F. Zheng and X.-S. Wan, Mechanism of Interaction between Bovine Serum Albumin and Sodium Dodecyl Sulfate, *Acta Phys.-Chim. Sin. (Wuli Huaxue Xuebao)*, 2013, **29** (12), 2639-2646 (8). DOI:10.3866/PKU.WHXB201310281.

43. E. Padrós, M. Duñach, A. Morros, M. Sabés and J. Mañosa, Fourth-Derivative Spectrophotometry of Proteins, *Trends Biochem. Sci.*, 1984, **9** (12), 508-510. DOI: 10.1016/0968-0004(84)90272-X.
44. G. Talsky, L. Mayring and H. Kreuzer, High-Resolution, High-Order UV/Vis Derivative Spectroscopy, *Photochem. Photobiol.*, 1978, **17** (11), 785-799. DOI: 10.1002/anie.197807853.
45. G. Azadi, A. Chauhan and A. Tripathi, Dilution of Protein-Surfactant Complexes: a Fluorescence Study, *Protein Sci.*, 2013, **22** (9), 1258-1265. DOI: 10.1002/pro.2313.
46. S. Jana, S. Ghosh, S. Dalapati and N. Guchhait, Exploring Structural Change of Protein Bovine Serum Albumin by External Perturbation Using Extrinsic Fluorescence Probe: Spectroscopic Measurement, Molecular Docking and Molecular Dynamics Simulation, *Photochem. Photobiol. Sci.*, 2012, **11** (2), 323-332. DOI: 10.1039/C1PP05180F.
47. K. Takeda, M. Miura and T. Takagi, Stepwise Formation of Complexes Between Sodium Dodecyl Sulfate and Bovine Serum Albumin Detected by Measurements of Electric Conductivity, Binding Isotherm, and Circular Dichroism, *J. Colloid Interface Sci.*, 1981, **82** (1), 38-44. DOI: 10.1016/0021-9797(81)90121-1.
48. M. S. Ali, N. Gull, J. M. Khan, V. K. Aswald, R. H. Khan and Kabirud-Dina, Unfolding of Rabbit Serum Albumin by Cationic Surfactants: Surface Tensiometry, Small-Angle Neutron Scattering, Intrinsic Fluorescence, Resonance Rayleigh Scattering and Circular Dichroism Studies, *J. Colloid Interface Sci.*, 2010, **352** (2), 436-443. DOI: 10.1016/j.jcis.2010.08.073.
49. T. Chakraborty, I. Chakraborty, S. P. Moulik and S. Ghosh, Physicochemical and Conformational Studies on BSA-Surfactant Interaction in Aqueous Medium, *Langmuir*, **25** (5), 2009, 3062-3074. DOI: 10.1021/la803797x.
50. F. Geng, L. Zheng, L. Yu, G. Li and C. Tung, Interaction of Bovine Serum Albumin and Long-chain Imidazolium Ionic Liquid Measured by Fluorescence Spectra and Surface Tension, *Process Biochem. (Oxford, U. K.)*, 2010, **45** (3), 306-311. DOI: 10.1016/j.procbio.2009.10.001.
51. M. A. Mir, N. Gull, J. M. Khan, R. H. Khan, A. A. Dar and G. M. Rather, Interaction of Bovine Serum Albumin with Cationic Single Chain+Nonionic and Cationic Gemini+Nonionic Binary Surfactant Mixtures, *J. Phys. Chem. B*, 2010, **114** (9), 3197-3204. DOI: 10.1021/jp908985v.
52. S. F. Santos, D. Zanette, H. Fischer and R. Itri, A Systematic Study of Bovine Serum Albumin (BSA) and Sodium Dodecyl Sulfate (SDS) Interactions by Surface Tension and Small Angle X-ray Scattering, *J. Colloid Interface Sci.*, 2003, **262** (2), 400-408. DOI: 10.1016/S0021-9797(03)00109-7.
53. E. L. Gelamo, R. Itri, A. Alonso; J. V. da Silva and M. Tabak, Small-angle X-ray Scattering and Electron Paramagnetic Resonance Study of the Interaction of Bovine Serum Albumin with Ionic Surfactants, *J. Colloid Interface Sci.*, 2004, **277** (2), 471-482. DOI: 10.1016/j.jcis.2004.04.065.
54. E. Lissi, C. Calderón and A. Campos, Evaluation of the Number of Binding Sites in Proteins from their Intrinsic Fluorescence: Limitations and Pitfalls, *Photochem. Photobiol.*, 2013, **89** (6), 1413-1416. DOI: 10.1111/php.12112.
55. T. N. Tikhonova, E. A. Shirshin, G. S. Budylin, V. V. Fadeev and G. P. Petrova, Assessment of the Europium(III) Binding Sites on Albumin Using Fluorescence Spectroscopy, *J. Phys. Chem. B*, 2014, **118** (24), 6626-6633. DOI: 10.1021/jp501277z.
56. M. van de Weert and L. Stella, Fluorescence Quenching and Ligand Binding: A Critical Discussion of a Popular Methodology, *J. Mol. Struct.*, 2011, **998** (1-3), 144-150. DOI: 10.1016/j.molstruc.2011.05.023.
57. W. L. Butler, Fourth Derivative Spectra, *Methods Enzymol.*, 1979, **56**, 501-515. DOI: 10.1016/0076-6879(79)56048-0.
58. A. Savitzky and M. Golay, Smoothing and Differentiation of Data by Simplified Least Squares Procedures, *Anal. Chem.*, 1964, **36** (8), 1627-1639. DOI: 10.1021/ac60214a047.
59. E. Padrós, A. Morros, J. Mañosa and M. Duñach, The State of Tyrosine and Phenylalanine Residues in Proteins Analyzed by Fourth-Derivative Spectrophotometry, *Eur. J. Biochem.*, 1982, **122** (1), 117-122. DOI: 10.1111/j.1432-1033.1982.tb06844.x.
60. B. Ojha and G. Das, Role of Hydrophobic and Polar Interactions for BSA-amphiphile Composites, *Chem. Phys. Lipids*, 2011, **164** (2), 144-150. DOI: 10.1016/j.chemphyslip.2010.12.004.
61. J. Tian, Y. Zhao, X. Liu and S. Zhao, A Steady-State and Time-Resolved Fluorescence, Circular Dichroism Study on the Binding of Myricetin to Bovine Serum Albumin, *Luminescence*, 2009, **24** (6), 386-393. DOI: 10.1002/bio.1124.
62. Y. Engelborghs, Correlating Protein Structure and Protein Fluorescence, *J. Fluoresc.*, 2003, **13** (1), 9-16. DOI: 10.1023/A:1022398329107.
63. Y. Engelborghs, The Analysis of Time Resolved Protein Fluorescence in Multi-tryptophan Proteins, *Spectrochim. Acta, Part A*, 2001, **57** (11), 2255-2270. DOI: 10.1016/S1386-1425(01)00485-1.
64. O. Julien, G. Wang, A. Jonckheer, Y. Engelborghs and B. D. Sykes, Tryptophan Side Chain Conformers Monitored by NMR and Time-Resolved Fluorescence Spectroscopies, *Proteins: Struct., Funct., Bioinf.*, 2012, **80** (1), 239-245. DOI: 10.1002/prot.23198.
65. X. Shen and J. R. Knutson, Subpicosecond Fluorescence Spectra of Tryptophan in Water, *J. Phys. Chem. B*, 2001, **105** (26), 6260-6265. DOI: 10.1021/jp010384v.
66. A. G. Szabo and D. M. Rayner, Fluorescence Decay of Tryptophan Conformers, *J. Am. Chem. Soc.*, 1980, **102** (2), 554-563. DOI: 10.1021/ja00522a020.
67. F. W. J. Teale, The ultraviolet fluorescence of proteins in neutral solution, *Biochem. J.*, 1960, **76** (2), 381-388.
68. J. B. A. Ross, W. R. Laws, K. W. Rousslang and H. R. Wyssbrod, Tyrosine Fluorescence and Phosphorescence from Proteins and Polypeptides, *Top. Fluoresc. Spectrosc.*, 2002, **3**, 1-64. DOI: 10.1007/0-306-47059-4_1.
69. R. W. Cowgill, Fluorescence and Protein Structure: XIV. Tyrosine Fluorescence in Helical Muscle Proteins, *Biochim. Biophys. Acta, Protein Struct.*, 1968, **168** (3), 1968, 417-430. DOI: 10.1016/0005-2795(68)90175-X.
70. N. Vekshin, M. Vincent and J. Gallay, Tyrosine Hypochromism and Absence of Tyrosine-Tryptophan Energy Transfer in Phospholipase A₂ and Ribonuclease T₁, *Chem. Phys.*, 1993, **171** (1-2), 231-236. DOI: 10.1016/0301-0104(93)85146-Y.
71. M. Weissbluth, Hypochromism, *Q. Rev. Biophys.*, 1971, **4** (1), 1-34. DOI: 10.1017/S003358350000038X.
72. W. Bał, M. Sokółowska, E. Kurowska and P. Faller, Binding of Transition Metal Ions to Albumin: Sites, Affinities and Rates,

- Biochim. Biophys. Acta, Gen. Subj.*, 2013, **1830**, 5444-5455. doi:10.1016/j.bbagen.2013.06.018.
73. S. L. Guthans and W. T. Morgan, The Interaction of Zinc, Nickel and Cadmium With Serum Albumin and Histidine-rich Glycoprotein Assessed by Equilibrium Dialysis and Immunoabsorbent Chromatography, *Arch. Biochem. Biophys.*, 1982, **218** (1), 320-328. DOI: 10.1016/0003-9861(82)90350-2.
74. E. Ohyoshi, Y. Hamada, K. Nakata and S. Kohata, The Interaction Between Human and Bovine Serum Albumin and Zinc Studied by a Competitive Spectrophotometry, *J. Inorg. Biochem.*, 1999, **75** (3), 213-218. DOI: 10.1016/S0162-0134(99)00090-2.
75. S. Trisak, P. Doumgdee and B. M. Rode, Binding of Zinc and Cadmium to Human Serum Albumin, *Int. J. Biochem.*, 1990, **22** (9), 977-981. DOI: 10.1016/0020-711X(90)90203-F.
76. Z. Yongqia, H. Xuying, D. Chao, L. Hong, W. Sheyi and S. Panwen, Structural Studies on Metal-Serum Albumin. IV. The Interaction of Zn(II), Cd(II) and Hg(II) with HSA and BSA, *Biophys. Chem.*, 1992, **42** (2), 201-211. DOI: 10.1016/0301-4622(92)85010-2.
77. Z. Yongqia, W. Yuwen, H. Xuying, H. Jiesheng, H. Yunqin, L. Pong and S. Panwen, Chemistry Equilibrium dialysis of metal-serum albumin. I. Successive stability constants of Zn(II) -serum albumin and the Zn²⁺ -induced cross-linking self-association, *Biophys. Chem.*, 1994, **51** (1), 81-87.
78. S. Baroni, G. Pariani, G. Fanali, D. Longo, P. Ascenzi, S. Aime and M. Fasano, Thermodynamic Analysis of Hydration in Human Serum Heme – albumin, *Biochem. Biophys. Res. Commun.*, 2009, **385** (3), 385-389. DOI: 10.1016/j.bbrc.2009.05.075.
79. A. K. Shaw and S. K. Pal, Resonance Energy Transfer and Ligand Binding Studies on pH-induced Folded States of Human Serum Albumin, *J. Photochem. Photobiol. B*, 2008, **90** (3), 187-197. DOI: 10.1016/j.jphotobiol.2008.01.001.
80. K. Kalyanasundaram and J. K. Thomas, Environmental Effects on Vibronic Band Intensities in Pyrene Monomer Fluorescence and Their Application in Studies of Micellar Systems, *J. Am. Chem. Soc.*, 1977, **99** (7), 2039-2044. DOI: 10.1021/ja00449a004.
81. L. Antonov, Fourth Derivative Spectroscopy—a Critical View, *Anal. Chim. Acta*, 1997, **349** (1-3), 295-301. DOI: 10.1016/S0003-2670(97)00210-9.



42x40mm (300 x 300 DPI)